COMPARATIVE ANALYSIS OF VISU SHRINK AND PMD MODEL ON SAR IMAGES FOR SPECKLE NOISE REDUCTION

Kalaiyarasi Alagumani
Department of Electronics and Communication Engineering,
V.S.B. Engineering College, Karur District, Tamil Nadu, (India).
E-mail: mukalaiyarasi@gmail.com
ORCID: https://orcid.org/0000-0001-9306-2654

Perumal Balasubramani
Department of Electronics and Communication Engineering, Kalasalingam Academy of Research and Education,Virudhunagar District, Tamil Nadu, (India).
E-mail: palanimet@gmail.com
ORCID: https://orcid.org/0000-0003-4408-9396

Pallikonda Rajasekaran Murugan
Department of Electronics and Communication Engineering, Kalasalingam Academy of Research and Education, Virudhunagar District, Tamil Nadu, (India).
E-mail: m.p.raja@klu.ac.in
ORCID: https://orcid.org/0000-0003-4408-9396

Recepción: 11/11/2019 **Aceptación:** 09/02/2021 **Publicación:** 30/11/2021

Citación sugerida:
Alagumani, K., Balasubramani, P., y Murugan, P. R. (2021). Comparative analysis of VISU shrink and PMD model on SAR images for speckle noise reduction. *3C Tecnología. Glosas de innovación aplicadas a la pyme, Edición Especial,* (noviembre, 2021), 261-277. https://doi.org/10.17993/3ctecno.2021.specialissue8.261-277

ABSTRACT

Removing noise from original image is often the initial step in image analysis. The best de-noising technique should not be only reducing the noise, but do so without blurring or changing the location of the edges. Many approaches have been proposed for noise reduction. Speckle noise can be easily removed by simple method such as partial Differential Equations method (PDEs). In this paper, Perona-Malik Diffusion (PMD) models have been proposed and compared with VISU Shrinkage (VS) method. Although both the methods are seemed to be comparable with removing speckle noise, speckles are more visible to mages processed by VS method. The experimental results show that the PMD model obtains superior performance with the PSNR value of 61.90%, SSI of 0.40, EPI of 0.51 and SSIM of 69.05%. The PSNR value has been increased by 20.2% when compared with VS de-speckling method.

KEYWORDS

De-speckling, PDE, Synthetic Aperture Radar, VISU shrink, DWT.

https://doi.org/10.17993/3ctecno.2021.specialissue8.261-277

1. INTRODUCTION

Remote sensing images are captured by various sensors. The captured images are often degraded by speckle noise called multiplicative noise. Speckle is predominantly due to the meddling of the requiting wave of the transducer aperture. It is one of the most perilous commotions that amend the quality of Synthetic Aperture Radar (SAR) coherent images (Choi & Jeong, 2019) and decreases the potentiality of the images. Speckle noise in SAR image is broadly severe, precipitating difficulties for image interpretation. It is generated because of the coherent processing of backscattered signals from multiple distributed targets of the earth surface.

The speckle noise reduction is usually the initial step in the analysis of SAR images. There are a several de-noising filters such as average filter, mean filter, median filter, Lee filter, sigma filter, Lee-sigma filter, and wiener filter etc., which are used in the noise removal of SAR images. These filters reduce speckle noise by smoothing and sharpening the original image. Due to which some unavoidable blur has been introduced in the de-noised image, and also the main problem in using adaptive procedure techniques is the empirical choice of thresholds to determine the size of windows. To overcome the above cited drawbacks, PDEs based methods are used for de-speckling SAR images. The PDE algorithm is more efficient for de-speckling the SAR images effectively without blurring the edges of original SAR images.

2. RELATED WORKS

Various Second-Order PDE methods including the anisotropic model (Kriti, Virmani, & Agarwal, 2019; Shen Liu *et al.*, 2012) and the total variational model (Rudin & Osher, 1994; Morteza *et al.*, 2019) were developed for suppressing noise. In Kriti *et al.* (2019), Fuzzy Morphological Anisotropic Diffusion method was utilized for SAR image speckle noise reduction. In Shen Liu *et al.* (2012), the anisotropic diffusion filter was used to reduce the speckle noise in ultrasound images. This method produced blur at the edges of the de-speckled image. In Rudin & Osher (1994), total variation with free local constraints method was used for noise reduction. In Morteza *et al.* (2019), Nonlinear total variation-based model was developed for noise removal of the image. This method produced sharp edges at the

https://doi.org/10.17993/3ctecno.2021.specialissue8.261-277

de-noised images. In Ehsan *et al.* (2014), Complex diffusion method for image enhancement was proposed and compared with the second, fourth-order PDE and showed that the complex diffusion method offers better result when the noise is low. The performance of this method is declined when the noise level is high.

In Liu *et al.* (2012a), PDE with Auxiliary images were used to de-speckle the SAR image. Here, the auxiliary images were used as priors. Multispectral and hyperspectral images were used in this experiment. The major drawback of using second-order Partial Differential Equation is the procreation of blocking effect in the de-noised image (Liu, Lai, & Pericleous, 2014, Van Rie *et al.*, 2019). To reduce the block effect, the fourth-order PDE method was developed by replacing the gradient operator by the Laplacian operator and this method gives better results by reducing the block effect (You & Kaveh, 2000). In Didas (2004), and Didas, Weickert and Burgeth (2005), Higher-order PDE based noise removal were performed. The higher-order PDEs are not widely used in de-speckling of SAR images because of its complex numerical implementation and enormous computations.

This paper is further organized as follows. Section III explains the materials and methods used in this paper. Section IV gives the various performance metrics used for comparing the performance of both de-speckling method. Section V provides the results and discussion. Conclusion of this paper is given in Section VI.

3. MATERIALS AND METHODS

Speckle noise diminishes the look and quality of SAR images which in turn decreases the performances of SAR image processing and Analysis. Therefore, the noise must be suppressed before processing the SAR images using various image processing techniques like multiple-look processing, adaptive and non-adaptive filters, etc.

3.1. VISU SHRINKAGE

De-speckling using wavelet shrinkage method, reduce the speckle noise existing in the noisy image with conserving the textual and edge attributes of the image. VISU Shrinkage (VS) is one the wavelet shrinkage method. In VS, thresholding is performed by applying universal threshold (UT) and it is proposed by Donoho (1994). The block diagram of VS de-speckling

https://doi.org/10.17993/3ctecno.2021.specialissue8.261-277

method is shown in fig 1. In this method, no need to calculate the threshold value at every subband level. Initially, 2D-DWT is applied on the speckled SAR image where the image is separated into four subband regions namely LL LH, HL and HH (Chang, Yu, & Vetterli, 2000). Then UT soft thresholding is performed on the wavelet coefficients. There are two types of thresholding viz. Hard thresholding produce unwanted artifacts in the de-speckled images while soft thresholding yields visually pleasing images. In soft thresholding, the coefficients below UT are set to zero while important coefficients are replaced by UT value. The shrinkage of the wavelet co-efficient is given by (Donoho, 1994):

$$\lambda = \sigma^{Noise}\sqrt{2\log(n)} \tag{1}$$

where, σ^{Noise}, is the standard deviation of the noise and 'n' is the number of pixel elements in the image. While UT selection, it is most necessary to evaluate the standard deviation of the noise (σ^{Noise}) from the wavelet coefficients. It is obtained by using the below formula:

$$\sigma = \frac{MAD}{0.6745} \tag{2}$$

where, *MAD* is the median of the absolute values of the wavelet coefficients (HH band of speckled image). In this experiment, 0.4349 is used as the universal threshold. At last, compute the 2D-IDWT to get the de-speckled SAR image. This technique is simple and effective, it removes speckle noise co-efficient that is insignificant relative to UT. The UT tends to be high for large values of MAD, it over smoothens the speckled SAR image and affects many original images co-efficient along with speckle noise. Also, it has been observed that threshold value should be smaller value for soft thresholding (Bruce & Gao, 1996). For de-speckling of SAR images, VISU shrink does not adapt well to suppress:

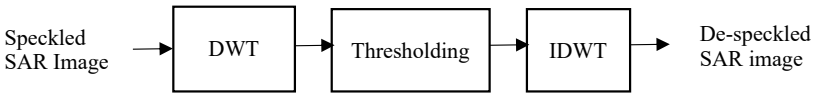

Figure 1. VISU Shrinkage (VS) De-speckling method.
Source: own elaboration.

https://doi.org/10.17993/3ctecno.2021.specialissue8.261-277

3.2. PMD MODEL

SAR images are affected by various noises which include both non-additive and additive noise. The non-additive ie, multiplicative noise in SAR image is otherwise called as speckle noise and it is defined as (Rafati *et al.*, 2016):

$$I(x,y) = f(x,y) * u(x,y) + n(x,y) \tag{3}$$

Where, *I (x,y)*, is the observed SAR image, *u (x,y)* is the multiplicative component of a speckled image, *n (x,y)* is the additive component of the speckled image. Since, the speckle noise is multiplicative, removing the speckle noise present in the remote sensing images is important. Only the multiplicative component is considered and the additional component is not to be considered. Therefore equation (3) can be rewritten as:

$$I(x,y) = f(x,y) * u(x,y) \tag{4}$$

The process used to de-speckle the SAR image using the PMD model is given in Figure 2. To convert the multiplicative component into the additive component, the log transform has been applied on both the sides of the above equation. Therefore, the above equation becomes,

$$S(x,y) = \log(I(x,y) = \log(f(x,y)) + \log(u(x,y)) \tag{5}$$

PMD model depends on heat diffusion equation which is defined as (Perona & Malik, 1990):

$$\frac{\partial S(x,y,t)}{\partial t} = \nabla.\left(c(x,y,t)\nabla S(x,y,t)\right) \tag{6}$$

Here, *S(x,y,t)* is the log transformed noisy SAR image, *c(x,y,t)* is the diffusivity, ∇ is the gradient operator, ∇ is the divergence operator. This equation was developed by Perona and Malik (1990). It can be expanded as:

$$\frac{\partial S(x,y,t)}{\partial t} = \nabla.\left(c(x,y,t)\nabla(\log(f(x,y)) + \log(u(x,y))\right) \tag{7}$$

This equation is more effective for suppressing the speckle noise while preserving the edge characteristics of the image. In this case, initially the gradient of the SAR image grad *x, grad y* is calculated in both x and y directions respectively. Then diffusivity is computed by using the below equation which is stated in (Khristenko *et al.*, 2019).

https://doi.org/10.17993/3ctecno.2021.specialissue8.261-277

$$c(x,y,t) = \frac{1}{1+\frac{|\nabla S|^2}{k^2}} \tag{8}$$

Here, k is a small constant used to control the diffusivity. It must be chosen between 5 to 100. The value of diffusivity:

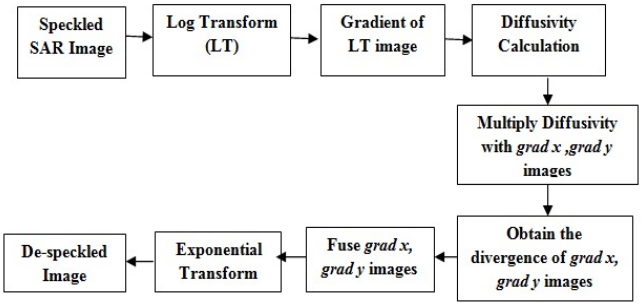

Figure 2. Work flow of PMD Model.
Source: own elaboration.

'*c*' changes at different regions of the image. The gradient of the image is high during the edges of the images, this leads to diffusivity has a small value. This consequently preserves the edges from smoothing. After that, the diffusivity is multiplied with the gradient image *grad x* and *grad* y images respectively. Thereafter, the divergence of *grad x* and *grad y* images are computed and both the images are fused to get the resultant divergence image. At last, take the exponential transform to get the de-speckled SAR image.

4. PERFORMANCE METRICS

To evaluate the performance improvement four different performance measures such as PSNR, SSI, EPI, and SSIM are enumerated based on the speckled SAR image and the de-speckled SAR image.

4.1 PEAK SIGNAL TO NOISE RATIO (PSNR)

PSNR is most widely used as a performance analyzing parameter. The higher value of PSNR gives a better quality of the de-speckled image. PSNR is defined as (Kalaiyarasi, Saravanan, & Perumal, 2016):

https://doi.org/10.17993/3ctecno.2021.specialissue8.261-277

$$PSNR = 10\log_{10}\frac{MAX_I^2}{MSE} \tag{9}$$

Where, MAX_I^2 is the maximum possible value of the original image. MSE is the mean square error, which must be lower value.

4.2 SPECKLE SUPPRESSION INDEX (SSI)

SSI is used to find the efficiency of the de-speckling algorithm, which is defined as (Dellepiane & Angiati, 2014):

$$SSI = \frac{\sqrt{Var(F)}}{Mean(F)} \cdot \frac{Mean(I)}{\sqrt{Var(I)}} \tag{10}$$

SSI should be the lowest value and the range lies between [0,1].

4.3 EDGE PRESERVATION INDEX (EPI)

Another parameter EPI can be computed by comparing the edges of the de-speckled image and the noisy SAR image. An efficient de-speckling method must have higher in Edge Preservation Index EPI (Ji & Zhang, 2017).

$$EPI = \frac{Gradient\ \ of\ \ the\ \ Filtered\ \ \text{Im}age\ \ Edges}{Gradient\ \ of\ \ the\ \ Noisy\ \ \text{Im}age\ \ Edges} \tag{11}$$

4.4 STRUCTURAL SIMILARITY INDEX MEASURE (SSIM)

When suppressing the speckle noise in SAR image processing, preserving edges is the most challenging one. Therefore, the additional parameters like EPI and SSIM have been evaluated here. SSIM is utilized to quantify the closeness amid the original SAR and the de-speckled SAR image. SSIM is define as (Nadernejad, Koohi, & Hassanpour, 2008):

$$SSIM = \frac{4\sigma_{xy}\overline{X}\overline{Y}}{\left(\sigma_x^2 + \sigma_y^2\right)\left[\left(\overline{X}\right)^2 + \left(\overline{Y}\right)^2\right]} \tag{12}$$

Where,

https://doi.org/10.17993/3ctecno.2021.specialissue8.261-277

$$\bar{X} = \frac{1}{N}\sum_{i=1}^{N} x_i \quad , \quad \bar{Y} = \frac{1}{N}\sum_{i=1}^{N} y_i$$

$$\sigma_x^2 = \frac{1}{N-1}\sum_{i=1}^{N}\left(x_i - \bar{X}\right)^2 \quad , \quad \sigma_y^2 = \frac{1}{N-1}\sum_{i=1}^{N}\left(y_i - \bar{Y}\right)^2$$

$$\sigma_{xy} = \frac{1}{N-1}\sum_{i=1}^{N}\left(x_i - \bar{X}\right)\left(y_i - \bar{Y}\right)$$

5. RESULTS AND DISCUSSION

Different SAR images have been used for this experiment which is shown in Figure 3.

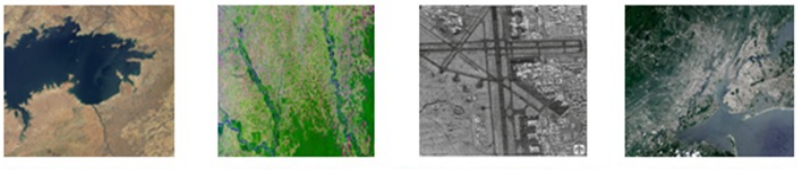

Figure 3. SAR images in different location. (a) Eastem Kariba, (b) Colombia Deforestation, (c) Airport SAR Image, (d) Ellis Island.
Source: own elaboration.

The de-speckled image using VS method is shown in Figure 4. In this method, noise reduction mainly depends on the UT value. The range of UT lies between 0 to 1. Here 0.4349 has been used as UT for thresholding the SAR image.

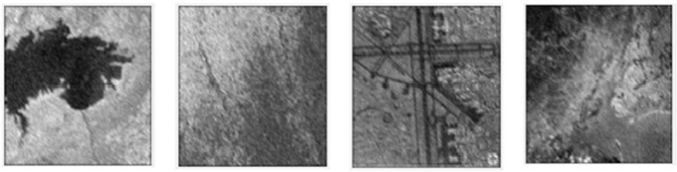

Figure 4. De-speckled SAR images using VS method. (a) Eastem Kariba, (b) Colombia Deforestation, (c) Airport SAR Image, (d) Ellis Island.
Source: own elaboration.

The de-speckled image using PMD model is shown in Figure 5. The VS method provides poor edge preservation. To overcome that, in PMD model the diffusivity plays an important role in preserving the edges of the images. The value of diffusivity co-efficient must be low for preserving the edges of the images. The obtained minimum and maximum value of

https://doi.org/10.17993/3ctecno.2021.specialissue8.261-277

diffusivity for different SAR images have been listed in Table 1. The gradient value will be high during the edges of the image. From equation (8), it can be noticed that diffusivity will be low when the gradient has a larger value. This technique is used to preserve the edges of the SAR images in the PMD model. The de-speckled image after the PMD model looks more cheerful, by eliminating the noise without affecting the edges and at the same time, it also reduces the block effect.

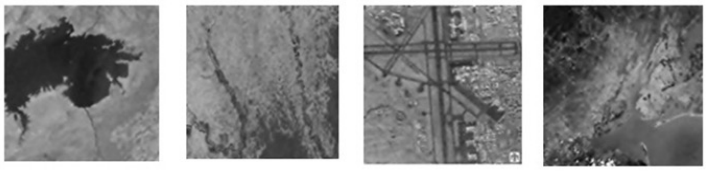

Figure 5. De-speckled SAR images using PMD model. (a) Eastem Kariba, (b) Colombia Deforestation, (c) Airport SAR Image, (d) Ellis Island.
Source: own elaboration.

From the above ocular results shown in Figures 4-5, it can be deduced that almost all speckle noise is removed, and the de-speckled image looks more comfortable without blocky effect. It is concluded that the PMD model has produced better visual images than the VS method.

Table 1. The minimum and maximum value of Diffusivity for SAR images.

Images	Minimum	Maximum
Eastem Kariba	0.0201	0.9997
Colombia Deforestation	0.0202	0.9952
Airport SAR Image	0.0108	0.9981
Ellis Island	0.0131	0.9972

Source: own elaboration.

https://doi.org/10.17993/3ctecno.2021.specialissue8.261-277

Table 2. Comparison of performance parameters of VS and PMD model.

S.No	Images	PSNR		SSI		EPI		SSIM	
		PMD	VS	PMD	VS	PMD	VS	PMD	VS
1	Eastem Kariba	62.17	42.36	0.39	0.23	0.56	0.37	66.84	53.29
2	Colombia Deforestation	61.88	39.96	0.36	0.28	0.68	0.60	61.44	55.18
3	Airport Image	59.93	40.63	0.36	0.26	0.46	0.36	62.21	50.28
4	Ellis Island	62.99	43.15	0.44	0.16	0.42	0.31	75.13	67.20
5	Wetland	64.64	42.80	0.43	0.10	0.50	0.34	74.70	67.73
6	Airborne SAR Image	63.16	40.81	0.41	0.16	0.50	0.53	70.22	50.54
7	Sea Ice	63.20	40.79	0.41	0.16	0.49	0.44	70.11	57.77
8	Barents Sea Ice Image	59.53	41.53	0.38	0.12	0.40	0.45	65.54	60.40
9	Arctic Sea Ice	60.91	39.51	0.44	0.11	0.47	0.42	75.58	63.34
10	Sea Ice MEASURES	62.62	42.13	0.37	0.15	0.38	0.39	63.28	57.59
11	Amazon_2010	56.92	42.54	0.40	0.28	0.50	0.36	68.67	59.29
12	Amazon_2020	64.03	44.57	0.45	0.27	0.67	0.22	77.11	53.22
13	Amazon_2030	63.95	42.63	0.43	0.25	0.55	0.35	74.09	62.17
14	Amazon_2040	61.62	42.27	0.41	0.19	0.67	0.38	69.74	55.54
15	Amazon_2050	60.96	39.84	0.35	0.24	0.50	0.47	61.16	52.45
	Average	61.90	41.70	0.40	0.19	0.51	0.39	69.05	57.73

Source: own elaboration

https://doi.org/10.17993/3ctecno.2021.specialissue8.261-277

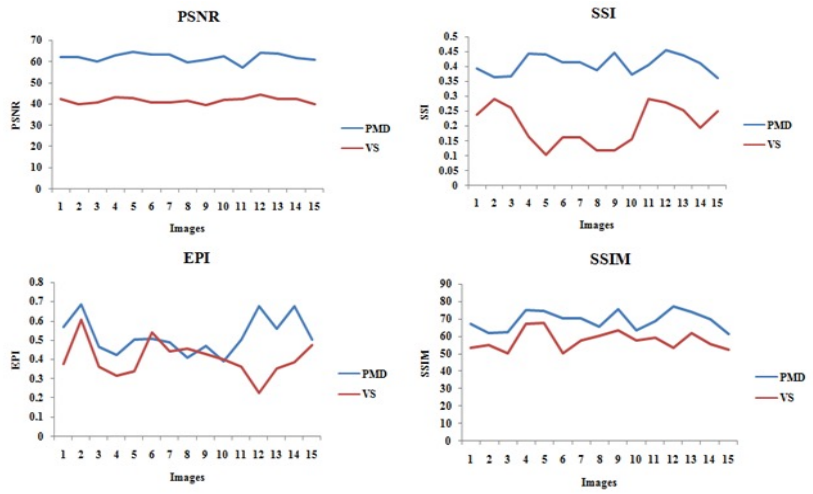

Figure 6. Graphical representation of PSNR, SSI, EPI and SSIM for VS method and PMD model.
Source: own elaboration.

Table 2 gives the comparison of performance parameters of VISU shrinkage and NSO-PDEs method on different SAR images respectively. From both the methods, VISU Shrink has the least performance as theoretically it uses a universal threshold for all sub-bands which is not optimal (Dixit *et al.*, 204). Figure 6 shows the comparison of PSNR, SSI, EPI, and SSIM for the two methods. From the four charts, it is inferred that the PMD model provides better PSNR, EPI, SSI and SSIM than VS method.

Table 3. Average Values of Performance Metrics.

Parameters	Methods	
	PMD	VS
PSNR	61.90	41.70
SSI	0.40	0.19
EPI	0.51	0.39
SSIM	69.05	57.73

Source: own elaboration.

The average values of performance metrics are given in Table 3. The average values have been calculated by taking the mean average values of total images used for this experiment. The graphical illustration of comparative analysis has been presented in Figure 7. From the graphical illustration analysis, it is noticed that the PMD de-speckling method produces

https://doi.org/10.17993/3ctecno.2021.specialissue8.261-277

better outcomes in terms of various performance metrics which includes PSNR of 61.90%, SSI of 0.40, EPI of 0.51 and SSIM of 69.05%.

Figure 7. Comparative analysis of Performance metrics of PMD and VS de-speckling methods. a) PSNR and SSIM, b) SSI and EPI.

Source: own elaboration.

6. CONCLUSIONS

PDE method has been most broadly used in SAR image processing particularly in suppressing speckle noise. In this paper, the PMD model has been proposed for speckle noise reduction. The performance of the PMD model is compared with the VISU shrinkage method. VS method follows the universal threshold scheme. This method does not minimize the mean

https://doi.org/10.17993/3ctecno.2021.specialissue8.261-277

squared error and it does not remove the speckle noise effectively. The experimental results show that the PMD model of speckle noise reduction yields a better result when compared to the VISU Shrinkage method. Additionally, the quality of the de-speckled image is better enhanced using the PMD model in terms of PSNR of 61.90%, SSI of 0.40, EPI of 0.51 and SSIM of 69.05%. The PSNR value has been increased by 20.2% when compared with the VS de-speckling method

ACKNOWLEDGMENT

We thank the Department of ECE of Kalasalingam Academy of Research and Education (Deemed to be University), Tamil Nadu, India for the computational facilities made available in Centre for Signal Processing Laboratory (Supported by Department of Science and Technology (DST), New Delhi under FIST Programme). (Reference No: SR/FST/ETI-336/2013 dated November 2013).

REFERENCES

Bruce, G., & Gao, H. (1996). Understanding Wave Shrink: Variance and bias estimation. *Biometrika, 83*, 727-745. https://doi.org/10.1.1.135.913

Chang, S. G., Yu, B., & Vetterli, M. (2000). Adaptive wavelet Thresholding for image denoising and compression. *IEEE Transactions on Image Processing, 9*(9), 1532-1546. https://ieeexplore.ieee.org/document/862633

Choi, H., & Jeong, J. (2019). Speckle Noise Reduction Technique for SAR images using Statistical Characteristics of Speckle Noise and Discrete Wavelet Transform. *Remote Sensing, 11*, 1-27. https://doi.org/10.3390/rs11101184

Dellepiane, S. G., & Angiati, E. (2014). Quality Assessment of Despeckled SAR Images. *IEEE Journal of Selected Topics in Applied Earth Observations and Remote Sensing, 7*(2), 691-707. https://ieeexplore.ieee.org/document/6595646

Didas, S. (2004). *Higher order variational methods for noise removal in signals and images* (Diploma thesis). Department of Mathematics, Saarland University, 2004. https://www.mia.uni-saarland.de/Theses/didas-dipl04.pdf

Didas, S., Weickert, J., & Burgeth, B. (2005). Stability and Local Feature Enhancement of Higher Order Nonlinear Diffusion Filtering. In Kropatsch W.G., Sablatnig R., Hanbury A. (eds) *Pattern Recognition. DAGM 2005*. Lecture Notes in Computer Science, vol 3663. Springer, Berlin, Heidelberg. https://doi.org/10.1007/11550518_56

Dixit, A., & Sharma, P. (2014). A Comparative Study of Wavelet Thresholding for Image Denoising. *International Journal of Image Graphics and Signal Processing, 12*, 39-46. http://www.mecs-press.org/ijigsp/ijigsp-v6-n12/IJIGSP-V6-N12-6.pdf

Donoho, D. L. (1994). Ideal spatial adaptation by wavelet shrinkage. *Biometrika, 81*(3), 425–455. https://doi.org/10.1093/biomet/81.3.425

Ji, X., & Zhang, G. (2017). Contourlet domain SAR image de-speckling via self-snake diffusion and sparse representation. *Multimedia Tools and Applications, 76*(4), 5873-5887. https://doi.org/10.1007/s11042-015-2560-2

Kalaiyarasi, M., Saravanan, S., & Perumal, B. (2016). A survey on: De-speckling Methods of SAR image. *Proceedings of International Conference on Control, Instrumentation, Communication and Computational Technologies (ICCICCT)*.

Khristenko, U., Scarabosio, L., Swierczynski, P., Ullmann, E., & Wohlmuth, B. (2019). Analysis of Boundary Effects on PDE-Based Sampling of Whittle--Matérn Random Fields. *SIAM/ASA Journal on Uncertainty Quantification, 7*(3), 948-974. https://doi.org/10.1137/18M1215700

Kriti, Virmani, J., & Agarwal, R. (2019). Effect of de-speckle filtering on classification of breast tumors using ultrasound images. *Biocybernetics and Biomedical Engineering, 39*(2), 536-560. https://doi.org/10.1016/j.bbe.2019.02.004

Liu, P., Huang, F., Li, G., & Liu, Z. (2012a). Remote-Sensing Image Denoising Using Partial Differential Equations and Auxiliary Images as Priors. *IEEE Geoscience and Remote Sensing Letters, 9*(3), 358-362. https://ieeexplore.ieee.org/abstract/document/6061940

Liu, S., Wei, J., Feng, B., Lu, W., Denby, B., Fang, Q., & Dang, J. (2012b). An anisotropic diffusion filter for reducing speckle noise of ultrasound images based on separability.

Proceedings of the 2012 Asia Pacific Signal and Information Processing Association Annual Summit and Conference (APSIPA ASC). https://ieeexplore.ieee.org/document/6411801

Liu, X. Y., Lai, C.-H., & Pericleous, K. A. (2014). A fourth-order partial differential equation denoising model with an adaptive relaxation method. *International Journal of Computer Mathematics, 92*(3). https://doi.org/10.1080/00207160.2014.904854

Nadernejad, E., Koohi, H., & Hassanpour, H. (2008). PDEs-Based Method for Image Enhancement. *Applied Mathematical Sciences, 2*(20), 981-993. https://www.researchgate.net/profile/Hamidreza-Koohi/publication/228653972_PDEs-Based_Method_for_Image_Enhancement/links/0c9605260d3508cda6000000/PDEs-Based-Method-for-Image-Enhancement.pdf

Perona, P., & Malik, J. (1990). Scale-space and edge detection using anisotropic diffusion. *IEEE Transactions on Pattern Analysis and Machine Intelligence, 12*(7), 629–639. https://ieeexplore.ieee.org/document/56205

Rafati, M., Arabfard, M., Zadeh, M. R. R., & Maghsoudloo, M. (2016). Assessment of noise reduction in ultrasound images of common carotid and brachial arteries. *IET Computer Vision, 10*(1), 1-8. https://doi.org/10.1049/iet-cvi.2014.0151

Rudin, L. I. & Osher, S. (1994). Total variation based image restoration with free local constraints. *IEEE International Conference on Image Processing, 1*, 31–35. https://ieeexplore.ieee.org/document/413269

Salehjahromi, M., Wang, Q., Gjesteby, L. A., Harison, D., Wang, G., & Yu, H. (2019). A directional TV based ring artifact reduction method. *Proceedings of SPIE 10948, Medical Imaging 2019, Physics of Medical Imaging, 109482C, 9,* https://doi.org/10.1117/12.2513037

Van Rie, J., Schütz, C., Gençer, A., Lombardo, S., Gasser, U., Kumar, S., Salazar-Alvarez, G., Kang, K., & Thielemans, W. (2019). Anisotropic Diffusion and Phase Behavior of Cellulose Nanocrystal Suspensions. *Langmuir, 35*(6), 2289-2302. https://doi.org/10.1021/acs.langmuir.8b03792

You, Y.-L., & Kaveh, M. (2000). Fourth-order partial differential equations for noise removal. *IEEE Transaction on Image Processing, 9*(10), 1723–1730. https://ieeexplore.ieee.org/document/869184

https://doi.org/10.17993/3ctecno.2021.specialissue8.261-277